Powdery mildew effectors AVR_{A1} and BEC1016 target the ER J-domain protein *Hv*ERdj3B required for immunity in barley

Running title: Two powdery mildew effectors target barley ERdj3B

Zizhang Li[1], Valeria Velásquez-Zapata[2,3], J. Mitch Elmore[3,4,#], Xuan Li[1], Wenjun Xie[1], Sagnik Banerjee[2,4], Hans J. L. Jørgensen[1], Carsten Pedersen[1], Roger P. Wise[2,3,5], Hans Thordal-Christensen[1]

[1)]Department of Plant and Environmental Sciences, University of Copenhagen, Thorvaldsensvej 40, 1871 Frederiksberg C, Denmark

[2)]Program in Bioinformatics & Computational Biology, Iowa State University, Ames, Iowa, 50011, USA

[3)]Department of Plant Pathology & Microbiology, Iowa State University, Ames, Iowa, 50011 USA

[4)] Department of Statistics, Iowa State University, Ames, Iowa, 50011, USA

[5)]Corn Insects and Crop Genetics Research Unit, USDA-Agricultural Research Service, Ames, Iowa, 50011, USA

Authors for correspondence: roger.wise@usda.gov and htc@plen.ku.dk

[#]Present Address: USDA-Agricultural Research Service, Cereal Disease Laboratory, 1551 Lindig Street, St. Paul, MN 55108, USA

ORCID IDs
Zizhang Li: 0000-0001-7818-5162
Valeria Velásquez-Zapata: 0000-0002-2756-2156
J. Mitch Elmore: 0000-0003-4068-0373
Xuan Li: 0000-0001-9338-0150
Wenjun Xie: 0000-0001-8101-5519
Sagnik Banerjee: 0000-0002-2052-7577
Hans J. L. Jørgensen: 0000-0002-5902-6550
Carsten Pedersen: 0000-0002-9520-2232
Roger P. Wise: 0000-0001-7786-1528
Hans Thordal-Christensen: 0000-0001-8813-0157

ABSTRACT

Plant disease resistance often occurs upon direct or indirect recognition of pathogen effectors by host nucleotide-binding leucine-rich-repeat (NLR) receptors. The barley powdery mildew fungus, *Blumeria graminis* f. sp. *hordei* (*Bgh*), secretes hundreds of candidate secreted effector proteins (CSEPs) to facilitate pathogen infection and colonization. One of these, CSEP0008, is directly recognized by the barley NLR, MLA1, and therefore designated AVR_{A1}. Here we show that AVR_{A1} and the sequence-unrelated *Bgh* effector BEC1016 (CSEP0491) suppress immunity in barley cells. We then used yeast 2-hybrid next-generation-interaction screens (Y2H-NGIS), followed by binary Y2H and bimolecular fluorescence complementation, to identify a common barley target of AVR_{A1} and BEC1016, the endoplasmic reticulum (ER)-localized J-domain protein, *Hv*ERdj3B. This is an ER protein quality control (ERQC) protein and silencing it increased the *Bgh* penetration rate in barley. *Hv*ERdj3B is localized to the ER lumen, and AVR_{A1} and BEC106 translocation into the ER was confirmed using a split GFP system. Together, these results suggest that the barley innate immunity, preventing *Bgh* entry into epidermal cells, is dependent on ERQC, which in turn is regulated by J-domain protein *Hv*ERdj3B and the two effectors. Previous work has shown that AVR_{A1} is directly recognized in the cytosol by the immune receptor, MLA1. We speculate whether the AVR_{A1} J-domain target being inside the ER, where it is inapproachable by NLRs, has forced the plant to evolve this challenging direct recognition.

INTRODUCTION

Plants have evolved a multilayered and interconnected innate immune system to protect themselves against pathogen attacks (Yuan et al., 2021a, Ngou et al., 2022). An initial layer, designated pathogen-associated molecular pattern-triggered immunity (PTI) is activated by pattern-recognition receptors (PRRs) located on the plasma membrane (PM) (Zipfel and Oldroyd, 2017). However, plant pathogens can secrete large numbers of effectors into the host to interfere with many host cellular processes in order to suppress PTI and establish parasitism (Kanja and Hammond-Kosack, 2020; Figueroa et al., 2021). In response, plants have evolved an additional interconnected system, termed effector-triggered immunity (ETI) that is initiated upon direct or indirect recognition of effectors by specific intracellular nucleotide-binding leucine-rich repeat

(NLR) receptors (Jones *et al.*, 2016; Thordal-Christensen, 2020; Ngou *et al.*, 2022). With some exceptions, NLR receptors represent the most utilized class of resistance proteins in agriculture (Sun *et al.*, 2020; van Wersch et al., 2020; Kourelis and van der Hoorn, 2018; Ngou et al., 2022). These innate immune systems rely on basic cellular processes, such as protein quality control systems. An intact endoplasmic reticulum (ER) quality control (ERQC) is required to transport certain *de novo* synthesized PRRs through the ER for them to be trafficked to their destination at the PM (Tintor and Saijo, 2014). For example, trafficking of the Arabidopsis EF-Tu receptor, EFR, is particularly dependent on the ERQC, where it requires the chaperones, ER DnaJ3B protein (ERdj3B) and binding immunoglobulin protein 3 (BiP3), as well as stromal cell-derived factor 2 (SDF2), for its proper folding and glycosylation (Nekrasov et al., 2009). ERdj3B is an ER luminal J-domain protein, but J-domain proteins elsewhere in the cell have been implicated in plant immunity as well. For instance, in rice infected by the blast fungus, *Magnaporthe oryzae*, cytosolic and mitochondria-associated J-domain proteins are essential for immunity, and interestingly, the latter protein is targeted by a disease-promoting, fungal effector (Zhong et al., 2018; Xu et al., 2020a). J-domain proteins are related to the bacterial DnaJ chaperones, also known as heat shock proteins 40 (HSP40). They interact with HSP70 proteins, such as BiP in the ER, to which they deliver misfolded client proteins and stimulate the HSP70 ATPase activity (Pobre et al., 2019; Fatima et al., 2021).

Several recent genomics, transcriptomics and proteomics studies have identified up to 600 candidates for secreted effector proteins (CSEPs) in the barley powdery mildew fungus, *Blumeria graminis* f. sp. *hordei* (*Bgh*) (Bindschedler et al., 2009; Spanu et al., 2010; Pedersen et al., 2012; Menardo et al., 2017; Frantzeskakis et al., 2018). However, only a subset of these have been studied in detail. Host-induced gene silencing (HIGS) analyses have demonstrated that approximately 20 CSEPs contribute to *Bgh* virulence, which is ~25% of those studied (Zhang et al., 2012; Pliego et al., 2013; Ahmed et al., 2015; 2016; Aguilar et al., 2016; Li et al., 2021; Yuan et al., 2021b). Li et al. (2021) screened ~100 CSEPs from *Bgh* and found 15 of them to suppress BAX-induced programmed cell death in *Nicotiana benthamiana*. Two of those, CSEP0139 and CSEP0182, also suppressed BAX-induced programmed cell death in barley. To date, only a few plant targets of *Bgh* effectors have been identified. CSEP0055 targets the barley defense proteins, PR1 and PR17 (Zhang et al., 2012), while CSEP0105 and CSEP0162 target the barley small heat

shock proteins, Hsp16.9 and Hsp17.5 (Ahmed et al., 2015). CSEP0064 and CSEP0264 target PR10, while CSEP0264, historically designated Blumeria effector candidate (BEC)1054, also targets eukaryotic elongation factor1 alpha (Pennington et al., 2019). In addition, CSEP0027 was recently found to target a barley catalase (Yuan et al., 2021b).

In addition to virulence functions, six *Bgh* CSEPs are directly recognized as avirulence proteins by NLRs encoded by an allelic series of the *Mla* powdery mildew resistance locus (Seeholzer *et al.* 2010; Lu et al., 2016; Saur et al., 2019; Bauer et al., 2021). For instance, CSEP0008 (gene ID BLGH_03023) is recognized by MLA1, and thus named AVR_{A1} (Lu et al., 2016). Other recognized CSEPs are CSEP0059 (AVR_{A7}), CSEP0174 (AVR_{A9}), CSEP0141 (AVR_{A10} and AVR_{A22}), and CSEP0372 (AVR_{A13}) (Lu et al., 2016; Saur et al., 2019; Bauer et al., 2021).

In this investigation, we were interested in discerning host targets for AVR_{A1} (CSEP0008, gene ID BLGH_03023) (Lu et al., 2016) and BEC1016 (CSEP0491, gene ID BLGH_07006) (Pliego et al. 2013), as examples of effectors with avirulence and virulence functions in barley-*Bgh* interactions, respectively. Recent advances in yeast 2-hybrid (Y2H) analyses, termed next-generation-interaction screening (NGIS) (Suter et al. 2015), use deep sequencing to score the output from Y2H screens (Erffelinck et al., 2018; Lewis et al., 2012, Pashkova et al., 2016; Trigg et al., 2017; Weimann et al., 2013; Yachie et al., 2016). These approaches facilitate a quantitative measure of which preys interact with each bait protein (Suter et al. 2015) and identify reproducible protein-protein interactions (PPI**)** with 70-90% accuracy (Pashkova et al., 2016; Trigg et al., 2017; Weimann et al., 2013; Velásquez-Zapata et al., 2021). This then allows functional PPI to be positioned within interactome networks (Mukhtar et al., 2011; Weßling et al., 2014; Velásquez-Zapata et al., 2021; 2022).

We used AVR_{A1} and BEC1016 as baits to conduct NGIS with a Y2H prey library developed from a barley-*Bgh* infection time course and identified the barley J-containing protein, *Hv*ERdj3B, as a host target for both effectors. Our analyses revealed that *Hv*ERdj3B is an ER-luminal protein and using a split GFP system we could show that both effectors translocate signal peptide (SP)-independently from the plant cytosol into the ER lumen. Silencing *Hv*ERdj3B, as well as overexpression of AVR_{A1} and BEC1016, enhanced the formation of fungal haustoria. Together, our results indicate an essential role of ERQC in barley innate immunity and suggest that *Bgh* effectors can interfere with ERQC processes.

RESULTS

AVR_{A1} and BEC1016 effectors contribute to *Bgh* infection

The two effector candidates AVR_{A1} (singleton) and BEC1016 (CSEP family 5) (Pedersen et al., 2012) are non-homologous in protein sequence, but both belong to the superfamily of RNase-like proteins associated with haustoria (RALPH) effectors with features resembling catalytically inactive RNases (Spanu, 2017) (**Supplemental Figure S1**). They were selected as examples of *Bgh* proteins with documented avirulence and virulence functions, respectively. As an avirulence protein recognized by MLA1, AVR_{A1} is predicted also to have virulence function. However, this could not be documented using HIGS, unlike the case for BEC1016 (Pliego et al., 2013). Both effectors display increased transcript abundance in compatible interactions on *mla6*-18982 mutant plants (Chapman et al., 2021) as compared to incompatible interactions on its resistant CI 16151 (*Mla6*) progenitor (**Supplemental Figure S2**), which supports their role in virulence. As an alternative approach to study virulence functions, we transiently over-expressed AVR_{A1} and BEC1016 (w/o SP) in leaf epidermal cells of one-week-old Golden Promise (susceptible) barley plants using particle bombardment. Two days later, the leaves were inoculated with *Bgh*, and after another 2 days transformed cells were scored for presence of a fungal feeding structure, termed haustorium, as evidence for successful penetration and fungal infection. Our data revealed that AVR_{A1} and BEC1016 significantly increased *Bgh* penetration, resulting in 96% and 150% higher haustoria numbers, respectively (**Figure 1A**).

Pathogen-induced callose depositions function as a chemical and physical reinforcement of the plant cell wall towards invading pathogens (Voigt, 2014). To determine whether AVR_{A1} and BEC1016 affect callose deposition, they were introduced into barley leaf cells using EtHAn, a strain of *Pseudomonas fluorescens* modified to express the type-3 secretion system (T3SS) (Thomas et al., 2009; Upadhyaya et al., 2014). To verify protein transfer to the barley cells, EtHAn transformed with a construct expressing β-glucoronidase (GUS) fused to a signal peptide for T3SS resulted in clear blue staining of the leaf cells after reaction buffer incubation (**Supplemental Figure S3**). While EtHAn itself triggers callose formation, it can at the same time be studied how this is

influenced by effectors (Sohn et al., 2007; Xu et al., 2020b). Five replicates of eight-day-old Golden Promise first leaves were infiltrated with EtHAn expressing GUS (negative control), AVR_{A1} or BEC1016. After 24 h, both the total number and total area of callose depositions were significantly reduced by the effectors (**Figure 1B**). Taken together, it appears that AVR_{A1} and BEC1016 target and inhibit PTI, and thereby promote *Bgh* penetration.

Both AVR_{A1} and BEC1016 interact with barley J-domain protein, *Hv*ERdj3B

To identify barley targets for AVR_{A1} and BEC1016, batch Y2H-NGIS was performed according to Velásquez-Zapata et al. (2021). The screens involved parallel histidine selection vs. non-selection and bait specificity to enrich for yeast cells expressing interacting bait and prey proteins. Sequencing reads across the GAL4 activation domain (AD) coding sequence into the prey protein coding sequences were performed on all cultures. We recently developed two complementary software packages, designated NGPINT and Y2H-SCORES, to quantify the outcome of Y2H-NGIS (Banerjee et al., 2021; Velásquez-Zapata et al., 2021). NGPINT facilitates the identification of GAL4 AD-prey *in-frame* coding sequence fusion reads. Then Y2H-SCORES uses count data to build a set of ranking scores to predict three properties expected from true interactors, *i.e.*, enrichment in selection vs. non-selection conditions, specificity to a bait screening, and *in-frame* selection of the prey (Velásquez-Zapata et al., 2021). Prey proteins that interact with the selected baits, as indicated by significant enrichment under selection, are reconstituted *in silico* with their mapped fusion reads to identify the complete prey sequence containing the PPI domain for further studies.

Using AVR_{A1} and BEC1016 effectors as baits to screen a 3-frame Y2H library made from our infection time course (Banerjee et al 2021; Velásquez-Zapata et al., 2021) we identified HORVU.MOREX.r2.1HG0019270, herein designated *Hv*ERdj3B, as a candidate interactor for both (**Figure 2**). A ranking (**Supplemental Table S1**) and visualization of the interactor candidates of each bait allowed the identification of a prey fragment covering the C-terminal two-thirds of *Hv*ERdj3B (aa 142-350). Binary Y2H according to Dreze *et al*. (2010) confirmed its interaction with AVR_{A1} and BEC1016 (**Supplemental Figure S4**).

To study the specificity of these interactions further, extensive binary Y2H assays were performed. The two effectors (w/o SP) were fused to either the Gal4 transcription factor DNA-binding domain (BD) or transcription-activation domain (AD) and combined with either the

full-length (w/o SP), the C-terminal two-thirds (aa 142-350) or the central part (aa 142-231) of *Hv*ERdj3B fused to either the AD or the BD. In both orientations of the setup, both effectors were found to interact with the C-terminal two-thirds and the central part, but not the full-length of *Hv*ERdj3B (**Figure 3)**. This suggests that the binding occurs only at the central part of *Hv*ERdj3B, and explains why reads did not appear from the 5' end of the coding sequence in the Y2H-NGIS sequencing results.

To confirm these interactions *in planta*, a bimolecular fluorescence complementation (BiFC) assay (Hu et al., 2002) was carried out in *N. benthamiana* leaf epidermal cells after Agrobacterium-mediated transformation. In this study, only the full-length *Hv*ERdj3B (w/o signal peptide) was used. GFP fluorescence signal was observed only when the *Hv*ERdj3B-cGFP fusion was combined with nGFP fused to the N-terminal or the C-terminal of the effectors (**Figure 4**). No GFP fluorescence was observed for any of the remaining six combinations for each effector (**Supplemental Figure S5**), supporting the specificity of the interactions.

Taken together, these results confirmed that the central portion (aa 142-231) of the J-domain protein *Hv*ERdj3B interacts with the diverged RALPH effectors AVR_{A1} and BEC1016. According to alignment with the most closely related mammalian J-domain protein this section corresponds very well with the predicted substrate-binding domain (Chen et al., 2017). *In planta*, however, this domain appears accessible for binding in the full-length *Hv*ERdj3B, which is a prerequisite for the interaction to be functionally relevant.

_Hv_ERdj3B is an ER luminal J-domain protein required for immunity during powdery mildew attack

HvERdj3B encodes a J-domain protein with an N-terminal signal peptide for ER targeting. The mature protein has a high amino acid identity of 77% to its closest Arabidopsis homologue, *At*ERdj3B, which is localized to the ER (Yamamoto et al., 2008). A strong accumulation of the *HvERdj3B* transcript was observed during *Bgh* penetration, peaking at 20 h after inoculation (**Supplemental Figure S2**), in line with an involvement in the immune response. Indeed, *At*ERdj3B has previously been implicated in immunity in Arabidopsis, where it is required for triggering of responses to the bacterial elongation factor-Tu (Nekrasov et al., 2009). To investigate whether *Hv*ERdj3B contributes to the immunity to *Bgh*, we silenced the *HvERdj3B* gene in barley plants

using transient-induced gene silencing (TIGS). Two RNAi constructs were generated with different *HvERdj3B* fragments and, together with a GUS reporter construct, bombarded into single epidermal cells of leaves of one-week-old Golden Promise leaves. Two days later, the leaves were inoculated with *Bgh* and formation of fungal haustoria was assessed after another 2 days. Our data revealed that silencing of *HvERdj3B* significantly enhances the penetration rate, as *HvERdj3B*-RNAi-1 and *HvERdj3B*-RNAi-2 on average tripled the number of haustoria (P value = 0.001). The *Mlo* RNAi positive control reduced the number of haustoria by ~40% (**Figure 5A**). This increase in the level of infection suggests that *Hv*ERdj3B plays an essential role in barley immunity.

To reveal *Hv*ERdj3B's subcellular localization, a C-terminal mYFP fusion of it (w. SP) was expressed in epidermal cells of barley leaves. Laser scanning confocal microscopy indicated that *Hv*ERdj3B is an ER protein as the mYFP signal has a reticulate pattern, which overlaps with the SP-mCherry-HDEL ER marker (**Figure 5B**). This localization of *Hv*ERdj3B found in barley was confirmed in *N. benthamiana* (**Supplemental Figure S6**). Next, we tested if *Hv*ERdj3B, as expected, is an ER luminal protein. Here we made use of a split GFP system different from BiFC. GFP is barrel-shaped and consists of 11 β-sheets (GFP1-11), which can be split into two fragments, β-sheets 1–10 (GFP1-10) and β-sheet 11 (GFP11). The two parts of GFP have affinity for one-another, and when they co-localize in the same compartment, a fluorescent GFP complex will be assembled (Xie et al., 2017). This was visualized as a reticulate GFP signal when the *Hv*ERdj3B-GFP11 fusion protein was co-expressed with an SP-GFP1-10-HDEL construct that delivers and retains GFP1-10 in the ER lumen (**Figure 5C**). No visible signal appeared when *Hv*ERdj3B-GFP11 was co-expressed with cytosolic GFP1-10 (**Figure 5E**). Furthermore, when GFP11-*Hv*ERdj3B without signal peptide was co-expressed with either SP-GFP1-10-HDEL or with cytosolic GFP1-10, GFP signal was absent and present, respectively (**Figure 5D,F**). In summary, these results show that *Hv*ERdj3B is important for barley immunity to *Bgh* and that it is located inside the ER lumen. This complements accumulating evidence of the role of ERQC and ERdj3B in plant immunity (Nekrasov et al., 2009; Tintor and Saijo, 2014).

AVR_{A1} and BEC1016 translocate from the plant cytosol to the ER lumen by unknown mechanism(s)

For interactions to occur between either AVR_{A1} or BEC1016, and *Hv*ERdj3B in barley epidermal cells attacked by *Bgh*, the two effectors are required to translocate from the fungus across either the plant plasma membrane or the extrahaustorial membrane into the plant cytosol; and then further across the plant ER membrane and into the ER lumen. Indirect evidence that AVR_{A1} translocates into the plant epidermal cell cytosol comes from the observation that it functions as an avirulence protein that binds to the cytosolic R-protein, MLA1, and triggers a hypersensitive response (HR) (Lu et al., 2016). It is assumed that BEC1016 also enters the plant epidermal cell, since the number of haustoria is increased when this effector is expressed in the epidermal cell cytosol after particle bombardment (Fig. 1A). To inquire whether both can translocate across the ER membrane, we started by over-expressing AVR_{A1}-GFP and BEC1016-GFP (both w/o signal peptide) in *N. benthamiana* epidermal cells. Here they were both localized to the cytosol and nucleus together with free mCherry, and no obvious ER signal could be distinguished as there was a complete overlap between the GFP and mCherry fluorescent signals (**Figure 6**). Expression in barley epidermal cells also suggested the effectors mainly to be cytosolic (**Supplemental Figure S7**).

However, to interact with *Hv*ERdj3B, the two effectors will have to enter the plant ER. To test this more rigorously, we again used our split GFP system (Xie et al., 2017). We generated constructs for fusing GFP11 to both the N and C-terminus of AVR_{A1}, BEC1016 and CSEP0105, all w/o SP. CSEP0105, which interacts with small heat shock proteins (Ahmed et al., 2015), was used as a negative control. These were then co-expressed with constructs for cytosolic GFP1-10 and ER-luminal SP-GFP1-10-HDEL in all combinations (**Figure 7**). GFP11 fused to the N and C-terminal of CNX^{TM}, the transmembrane domain of the ER membrane protein, calnexin 1 (Xie et al., 2017), was used as reference (**Figure 7A,B,I,J**). All three effectors combined with GFP1-10 resulted in cytosolic and nuclear GFP signal (**Figure 7C-H**). Yet, all combinations of AVR_{A1} and BEC1016 with SP-GFP1-10-HDEL in addition resulted in cells with distinct GFP signal from a reticulate network and the perinuclear space (**Figure 7K-N, Supplemental Figure S8**). Since this was never seen for CSEP0105 (**Figure 7O,P**) and since the ER-localized GFP11-CNX^{TM}/SP-GFP1-10-HDEL combination also gave reticulate network signal (**Figure 7I**), the data indicate that a fraction of the cytosolic AVR_{A1} and BEC1016 specifically translocate into the ER lumen post-translationally and independently of their signal peptides.

DISCUSSION

Powdery mildew fungi are obligate biotrophic pathogens that feed on living plant tissues for nutrient uptake via haustoria. To suppress host defenses and promote colonization, these pathogens deliver a large repertoire of effectors into host cells (Frantzeskakis et al., 2018). Therefore, identifying the host targets of these effectors and their function will lead to detailed understanding of how infection is established and maintained. We focused on *Bgh* AVR_{A1} and BEC1016, as examples of avirulence proteins and proteins having a detectable contribution to fungal virulence, respectively (Lu et al., 2016; Pliego et al., 2013). Here we found that bacterial T3SS-based delivery of these effectors reduced defense-associated callose deposition and that over-expression enhanced *Bgh* haustorial development. Through Y2H-NGIS, these effectors were found to target the same host protein, *Hv*ERdj3B, which we further substantiated through binary Y2H and BiFC assays. Silencing of the *HvERdj3B* gene in barley led to increased formation of *Bgh* haustoria, indicating that this ER protein is involved in the plant's immunity against fungal penetration.

It is well-documented that ER stress responses and ERQC contribute to plant immunity in several ways. Our data are consistent with a previous study showing that a T-DNA line mutated in *HvERdj3B*'s closest homologue in *Arabidopsis*, *AtERdj3B*, is more susceptible to bacterial pathogens (Nekrasov et al., 2009). Here it was reported that *At*ERdj3B is involved in PTI. In the ER, it forms a complex with SDF2 and the Hsp70 BiP1, which are required for proper trafficking and function of the plasma membrane leucine-rich-repeat receptor kinases, EFR. *Hv*ERdj3B may have a similar function and may be involved in proper functioning of PRRs in barley.

Besides being required for processing of pattern-recognition receptors, ERQC is required for secretion of antimicrobial proteins and linked to pathogen-induced programmed cell death (Li et al., 2009; Moreno et al., 2012; Qiang et al., 2012; Kørner et al., 2015). In addition, a recent study showed that the ER proteins, UBAC2 and PICC, interact with each other and are required for proper delivery of callose synthase to the plasma membrane and for flagellin-triggered callose deposition (Wang et al., 2019). As callose is important for immunity towards penetration by powdery mildew fungi (Voigt, 2016), it will be interesting to see if future studies can demonstrate

that the ERdj3B/BiP complex is required for UBAC2/PICC-dependent callose deposition. Therefore, even if ERdj3B is essential for maturation of certain PRRs in the ER, there might be additional ways by which it contributes to plant immunity and thus how *Bgh* uses AVR_{A1} and BEC1016 to aid the penetration process.

Since our immediate localization study suggested both effectors to be cytosolic and nuclear, while *Hv*ERdj3B was found to be ER-luminal, we used the split GFP system to demonstrate that these effectors are also translocated into the ER. There are other studies showing that pathogen effectors enter the ER to facilitate infection by targeting ER-localized host proteins. For instance, the RXLR effector PcAvr3a12 from the *Arabidopsis* pathogen, *Phytophthora capsici*, can post-translationally enter the ER and target the ER-localized host PPIase, FKBP15-2, which is involved in ER stress-sensing and required for ER stress-mediated plant immunity (Fan et al., 2018). Furthermore, it has been reported that an essential effector, PsAvh262, secreted by the soybean pathogen, *P. sojae*, translocates from the host cytosol into the ER to stabilize BiPs, thereby suppressing ER stress-triggered cell death and facilitating infection (Jing et al., 2016). In both cases, it was shown by BiFC that effector-target interactions occur inside the ER. Yet another recent study showed that a nematode effector (CLE) is translocated from the plant cell cytosol to the ER, and then secreted as an extracellular receptor ligand (Wang et al., 2021). Here post-translational ER uptake was demonstrated using the GFP1-10/11 system, which we also used. Together these observations suggest that these effectors hijack one or more signal peptide-independent plant ER uptake mechanisms.

AVR_{A1} and BEC1016 both interact with *Hv*ERdj3B and both enter the ER post-translationally and signal peptide-independently. Yet they have very diverse amino acid sequences. However, the two effectors appear derived from an ancient RNAse, and they are potentially structurally related (Pedersen et al., 2012), which may explain the shared functions. Interestingly, the ERQC machinery is known to engage in the post-translational ER protein uptake through the Sec61 translocon complex (Zimmermann et al., 2021). Thus, we consider that interactions of AVR_{A1} and BEC1016 with *Hv*ERdj3B may facilitate one-way movement through this translocon into the ER lumen. Previously, we found that silencing of the barley Sec61 β- and γ-subunits both reduce the plant's susceptibility to *Bgh* (Zhang et al., 2013; Xu et al., 2015). These findings were difficult to explain as preventing ER uptake of immunity-associated proteins, such as

PR-proteins and PM-bound PRR should increase the plant susceptibility. However, our present finding of a susceptibility suppressing role AVR_{A1} and BEC1016 (Fig. 1), which both enter the ER, may make the consequences of Sec61 (Zhang et al., 2013; Xu et al., 2015) more meaningful.

Often effectors are recognized indirectly by NLRs after they have impacted effector targets, which are guarded and associated with the NLRs (Carter et al., 2019; Ngou et al., 2022; Thordal-Christensen, 2020). However, an effector target that contributes to immunity, like *Hv*ERdj3B, inside the ER may not be guarded by an NLR, as to date, such receptors have not been localized in this compartment. Instead, this favors a requirement for direct effector monitoring by NLRs in the cytosol, which agrees with the direct recognition and interaction of AVR_{A1} and the NLR, MLA1 (Lu et al., 2016). One may speculate whether targeting an ER luminal host protein thus has provided an evolutionary benefit to the pathogen, since it may be more demanding for the plant to invent specific recognition of each effector, rather than guarding proteins targeted by more effectors potentially from different pathogens.

MATERIAL AND METHODS

Plant and Fungal Materials

Seedlings of barley (*Hordeum vulgare* L.) cv. 'Golden Promise' were grown at 16 h light (150 µE s^{-1} m^{-2}, 20°C) / 8 h of darkness (20°C) to be used for inoculations, gene amplifications, transient-induced gene silencing (TIGS), overexpression, and callose deposition assays after effector-delivery using EtHAn. *Blumeria graminis* f. sp. *hordei* (*Bgh*) isolate C15 was propagated on barley P-02 plants in a cycle of 1 week. Four to six-week-old *Nicotiana benthamiana* plants were used for BiFC and subcellular localization studies after Agrobacterium-mediated leaf cell transformation.

Gateway Plasmid Construction

Coding DNA sequences (CDS) for the effectors, AVR_{A1} and BEC1016, w/o their signal peptides, were amplified using primer pairs listed in **Supplemental Table S2**. PCR was performed on cDNA from barley leaves infected with *Bgh*, and the fragments were cloned into pENTR/D-TOPO® vectors (Invitrogen), with or without stop codons. The CDS for the full-length barley *Hv*ERdj3B (HORVU1Hr1G022990) with stop codon was synthesized by TWIST Bioscience (San Francisco, CA, USA). Fragments of *Hv*ERdj3B were amplified therefrom using primers listed **Supplemental Table**

S2 and cloned into pENTR/D-TOPO. Subsequently, the entry clone inserts were transferred to destination vectors using Gateway LR cloning reactions (Invitrogen). RNAi constructs were generated in the 35S promoter-driven hairpin destination vector, pIPKTA30N (Douchkov et al., 2005). The *Hv*ERdj3B-RNAi-1 and -2 constructs contain *Hv*ERdj3B CDS fragments from positions 283 to 579 and 532 to 879, respectively. These sequences were predicted using the si-Fi open-source software (Lück et al., 2019). For over-expression constructs, the CDSs for *Hv*ERdj3B (with signal peptide), AVR_{A1} and BEC1016 (w/o signal peptides) were transferred into pUbi-mYFP-GW-Nos and pUbi-GW-Nos destination vectors. All the constructs were sequenced for confirmation.

Barley Single Cell Transient-Induced Gene Silencing and Over-Expression

Barley leaf epidermal cell transformation was obtained after particle bombardment as described by Douchkov et al. (2005) and Nowara et al. (2010), using the biolistic PDS-1000/He Particle Delivery System from Bio-Rad. For each bombardment, six detached 1st leaves of one-week-old Golden Promise barley plants were used. The particle coating was performed using 7 µg of DNA for each construct together with 2.4 mg of gold, 1 µg μl^{-1} of protamine (Sivamani et al, 2009) and 0.625 M $CaCl_2$ (Rasco-Gaunt et al., 1999). For the bombardments, a hepta adapter and rupture discs bursting at a helium pressure of 1.100 psi were used. After bombardment, the leaves were transferred onto 1% phytoagar petri dishes containing 40 mg ml^{-1} benzimidazole. For TIGS, the constructs were co-transformed with a GUS reporter gene construct driven by the pUbi promoter into the epidermal cells. Two days later, the leaves were inoculated with *Bgh*, and after another 2 days, they were stained for GUS activity. Transformed (blue) cells were assessed microscopically for the presence of haustoria as an indication of fungal infection. The haustorium formation rate was calculated as the number of blue cells with haustoria divided by the total number of blue cells. An mYFP and the empty vector pIPKTA30N were used as negative controls and the Mlo RNAi (pIPKTA36) (Douchkov et al., 2005) construct was used as positive control. The effect of constructs was analysed by a logistic regression model with random effects, assuming a binominal distribution, with construct as fixed effect and the experiment × construct × leaf interaction as random effect. The analyses were performed in PC-SAS (release 9.4, SAS Institute, Cary, NC). The SP-mCherry-HDEL construct was from Nelson et al. (2007).

***Agrobacterium tumefaciens* infiltration-mediated transformation of *Nicotiana benthamiana* leaf cells**

T-DNA construct were introduced into *A. tumefaciens* strain GV3101 by electroporation. The transformed bacterial cells were grown on LB agar plates supplemented with Rifampicin, Spectinomycin and Gentamycin antibiotics. For leaf cell transformation, over-night liquid cultures (28°C) of recombinant *A. tumefaciens* were harvested by centrifugation and resuspended in 10 mM $MgCl_2$, 10 mM MES and 200 µM acetosyringone to OD_{600}=0.6. A strain of *A. tumefaciens* with a construct expressing the p19 silencing suppressor (Voinnet et al., 2003) was managed the same way. The resuspended *A. tumefaciens* transformants, including the one with the P19 construct, were mixed in equal ratios and infiltrated into leaves of four to six-week-old *N. benthamiana*.

Yeast 2-Hybrid, Next-Generation-Interaction Screen

The *Bgh* effectors AVR_{A1} and BEC1016 were used as baits in Y2H-NGIS to mine for novel protein interactions. Bait sequences (w/o signal peptides) were fused with the GAL4 transcription factor binding domain (GAL4-BD) in the p97-BD, Leu2p vector and transformed into *Saccharomyces cerevisiae* strain Y8930 (Dreze et al., 2010). Pooled mRNA from an infection time course of the resistant barley line CI 16151 (*Mla6*) and four fast-neutron-derived mutants inoculated with *Bgh* isolate 5874 (AVR_{a1}, AVR_{a6}) (Surana, 2017; Chapman et al. 2021), was used to prepare a three-frame cDNA prey library in the Gateway-compatible ARS4/CEN6 GAL4 activation domain (AD) vector, p86-AD, Trp1p (Dreze et al. 2010; Yu et al. 2015). After transforming the library into *S. cerevisiae* strain Y8800, 1.1 x 10^7 primary clones were mated with each bait clone and subsequently cultured in three replicates under two conditions (selection and non-selection). At the end of each culture, prey plasmids were isolated, and the prey cDNA fragments were amplified by PCR. Amplicons were sent for sequence analysis using the Illumina HiSeq 2500 platform at the Iowa State University sequencing facility, collecting 5–10 million reads per sample. Y2H-NGIS data from these experiments were analyzed using the NGPINT and Y2H-SCORES software (Banerjee et al., 2021; Velásquez-Zapata et al., 2021) to reconstruct the prey fragments and rank them as interactors of each bait. Outputs from these pipelines allowed us to identify interacting prey fragments, their frame with the Gal4-AD as well as enrichment and specificity scores that assess their properties as Y2H interactors.

Binary Yeast 2-Hybrid Assay

Using the output from the Y2H-NGIS, we designed primers to re-clone identified prey fragments into p86-AD to confirm interactions using binary Y2H (Dreze et al., 2010) under three levels of selective media: Diploid selection (SC-LW), interaction selection (SC-LWH) and specific selection (SC-LWH + 0.1 mM 3-AT) using three dilutions (10^0, 10^{-1}, 10^{-2}) as shown in **Supplemental Figure S4**. After the first confirmation of *Hv*ERdj3B as prey, new AVR_{A1}, BEC1016 and *Hv*ERdj3B constructs were made in the destination vectors pDEST-AS2-1 (GAL4-BD) and pDEST-ACT2-1 (GAL4-AD) (Robertson, 2004). These constructs were transformed into the haploid yeast strains, Y189 and Y190, respectively. Subsequent matings, selections and *LacZ* reporter assays were made according to the Matchmaker Gold Yeast Two-Hybrid System user manual (Clontech; Mountain View, Ca, USA).

Bimolecular Fluorescence Complementation Assay

The CDS for full-length barley *Hv*ERdj3B and both effectors, w/o signal peptides, and with and w/o stop codons, were transferred to 35S promoter-driven BiFC binary destination vectors (Kamigaki et al. (2016) as N- and C-terminal fusions of nGFP (aa 1 to 174) and cGFP (aa 175 to 239). Two-by-two combinations of constructs were transformed into *N. benthamiana* leaves by *A. tumefaciens* infiltration. Two days after infiltration, the fluorescence signals of all eight possible AVR_{A1}/*Hv*ERdj3B combinations and of all eight possible BEC1016/*Hv*ERdj3B combinations were evaluated by a laser scanning confocal microscopy.

Localization of Effectors in the ER

The GFP1-10/GFP11 split GFP system (Xie et al., 2017) was used to document presence of effectors in the ER lumen. CDS for the effectors AVR_{A1} and BEC1016, w/o their signal peptides, were transferred to the T-DNA Gateway destination vectors, pGFP11-GW and pGW-GFP11, to fuse them to GFP11. T-DNA constructs for GFP11-CNX™ and CNX™-GFP11 were from Xie et al. (2017). These were co-expressed with constructs for cytosolic GFP1-10 and ER-luminal SP-GFP1-10-HDEL from Xie et al. (2017).

Callose Deposition Assay

CDSs for the GUS reporter gene and both CSEPs, w/o signal peptides and with stop codons were transferred to the AvrRPS4 promoter-driven destination vector, pEDV6 (Fabro et al., 2011), and transformed into *Pseudomonas fluorescens* EtHAn (Thomas et al., 2009) by electroporation. Transformed EtHAn strains were grown over-night in King's B medium containing ampicillin, chloramphenicol, tetracycline and gentamicin at 28°C. The bacteria were harvested by centrifugation and resuspended in 10 mM $MgCl_2$ to a final OD_{600}=0.3 and infiltrated into leaves of eight-day-old barley. Twenty-four hours later, the callose response was assayed in the infiltrated leaf areas by aniline blue fluorescence using a Nikon ECLIPSE Ni-U fluorescence microscope. For one repeat, ten 1110 µm x 740 µm (5184 × 3456 pixels) images from random sites at one leaf were used to quantify the number of callose deposits and the accumulated area of callose deposits using the Fiji open-source platform (Schindelin et al., 2012, Jin and Mackey, 2017). The outcomes of effectors were calculated relative to GUS as control and analysis of the callose deposition data was performed for the total number and area of the callose deposits independently. We performed a repeated measures ANOVA (Keselman et al., 2001) to test the effect of the treatments considering the repeated measures by leaf. Significant treatments effects were further explored with a paired-sample t test and the *P* values were adjusted using the method of Benjamini and Hochberg (1995).

Differential transcript accumulation

RNA-Seq data were extracted from an infection time course of barley CI 16151 and the derived fast-neutron mutant, *mla6*-m18982, at 0, 16, 20, 24, 32, and 48 hours after inoculation with *Bgh* isolate 5874 (AVR_{a1}, AVR_{a6}) (5 genotypes × 6 time points × 3 biological replications; NCBI-GEO GSE101304) and analyzed as described in (Chapman et al., 2021; Hunt et al., 2019). Genes were differentially expressed at an adjusted *P* of < 0.001 for barley and < 0.003 for *Bgh* were considered significant.

Availability of Y2H-NGIS code, data, and materials

Infection-time-course RNA-Seq data are at NCBI-GEO under the accession number GSE101304 (https://www.ncbi.nlm.nih.gov/gds/?term=GSE101304). R code and the ReadMe file for the

NGPINT and Y2H-SCORES software used to identify *Bgh* AVR_{A1} and BEC1016 interactors are provided at the GitHub page (https://github.com/Wiselab2/). Raw Y2H-Seq reads are at NCBI-GEO under accession numbers GSE164954 (AVR_{A1}/CSEP0008) and GSE166108 (BEC1016/CSEP0491).

The following supplementary material is available:

Supplemental Figure S1. Attempted alignment of the amino acid sequences of AVR_{A1} (CSEP0008, BLGH_03023) and BEC1016 (CSEP0491, BLGH_07006).

Supplemental Figure S2. Transcript accumulation on barley inoculated with *Bgh* isolate 5874.

Supplemental Figure S3. EtHAn-delivery of β-glucuronidase into barley leaf cells.

Supplemental Figure S4. Y2H used to validate interactions between AVR_{A1}, BEC1016 and *Hv*ERdj3B

Supplemental Figure S5. Bimolecular fluorescence complementation study of the interaction between AVR_{A1}, BEC1016 and *Hv*ERdj3B.

Supplemental Figure S6. Subcellular localization of *Hv*ERdj3B in *N. benthamiana* epidermal cells.

Supplemental Figure S7. Localization of AVR_{A1} and BEC1016 in barley leaf epidermal cells.

Supplemental Figure S8. BEC1016 can translocate into the ER.

Supplemental Table S1. Y2H-SCORES for the AVRA1 and BEC1016 baits.

Supplemental Table S2. Primer sequences for plasmid constructions (5´ to 3´)

ACKNOWLEDGMENTS

We thank the late Dr. Patrick Schweizer (Leibniz Institute of Plant Genetics and Crop Plant Research, Gatersleben, Germany) for providing the RNAi vector and the Mlo RNAi construct, Dr. Masumi Robertson (Commonwealth Scientific and Individual Research Organization Plant Industry) for the Gateway Y2H vectors (pDEST-ACT2 and pDEST-AS2-1), Greg Fuerst (USDA-ARS at Iowa State University) for conducting the *Bgh* time-course infection experiment and expert isolation of RNA for the 3-frame Y2H library, Associate Professor Shoi Mano for the BiFC-vectors, and Drs. Pietro Spanu (Imperial College, U.K.) and Ralph Panstruga (RWTH Aachen, Germany) for CSEP clones. Research supported in part by China Scholarship Council for PhD-student scholarship 201708340064 to ZZ, Novo Nordisk Foundation Challenge grant NNF19OC0056457 to HTC, Villum Fonden Experiment Programme grant 00028131 to HTC, Fulbright - Minciencias 2015 & Schlumberger Faculty for the Future fellowships to VVZ, USDA-ARS Postdoctoral Research

Associateship and USDA-NIFA-ELI Postdoctoral Fellowship 2017-67012-26086 to JME, Oak Ridge Institute for Science and Education under U.S. Department of Energy contract number DE-SC0014664 to SB, and National Science Foundation - Plant Genome Research Program grant 13-39348, USDA-National Institute of Food and Agriculture grant 2020-67013-31184 and USDA-Agricultural Research Service project 3625-21000-067-00D to RPW. The funders had no role in study design, data collection and analysis, decision to publish, or preparation of the manuscript. Mention of trade names or commercial products in this publication is solely for the purpose of providing specific information and does not imply recommendation or endorsement by the CSC, NNF, VF, USDA, NIFA, ARS, DOE, ORAU/ORISE or NSF. USDA is an equal opportunity provider and employer.

Author contributions

ZL: Transient effector OE and haustorial formation rate, extensive binary Y2H, protein subcellular localizations, contributed to writing

VVZ: Y2H-NGIS, developed the Y2H-SCORES software to rank high-priority candidates, identified *Hv*ERdj3B, and validated by first binary Y2H, contributed to statistics, contributed to writing,

JME: Initiated the overall concept and experimental plan. Constructed the 3-frame barley/Blumeria Y2H library and developed Y2H-NGIS screen.

XL: Callose response to EtHAn infiltrations

WX: Assisted and supervised subcellular localizations

SB: Developed the NGPINT software and analyzed sequence count data.

HJLJ: Contributed to statistics

CP: Supervised and contributed to writing

RPW: Initiated the overall concept and experimental plan, organized, supervised and contributed to writing

HTC: Organized and supervised the work, wrote first draft, lead the writing and finalized the work

Figure and table legends

Figure 1. Influence of AVR_{A1} and BEC1016 on *Bgh* infection and callose deposition in barley. A, Effect of transient over-expression of AVR_{A1} and BEC1016 on *Bgh* invasion. pUbi promoter-driven over-expression constructs were co-bombarded with a GUS-reporter constructs into leaf epidermal cells of 1-week-old barley and 2 days later inoculated with *Bgh*. After another 2 days, the fungal haustorium formation was scored in GUS expressing cells. Data shown are mean values

of three independent experiments. Error bars, SE. Letters (a, ab and b) indicate significant differences calculated using a logistic regression model (P = 0.0179). **B,** AVR_{A1} and BEC1016 can reduce bacterium-triggered callose deposition in barley plants estimated as numbers of callose spots (left) and area of callose spots (right). Leaves of eight-day-old barley plants were infiltrated with EtHAn, transformed with pEDV6-GUS, pEDV6-AVR_{A1} or pEDV6-BEC1016, and 24 h later the callose deposition we scored. Boxplots for the total number and total area of callose depositions show data for all pictures taken across biological replicates (one replicate = ten pictures from each of three leaves, ie. 30 pictures) under each treatment. A repeated measures ANOVA followed for a paired sample t test were used to compare the treatments. ***, $P < 2x10^{-16}$. Data shown are based on five independent experiments, statistically treated as replicates.

Figure 2. Y2H-NGIS used to identify interactions between AVR_{A1}, BEC1016 and *Hv*ERdj3B. A, *Hv*ERdj3B gene model with exons depicted as blue boxes and introns as hash marks. **B,** Integrative genomic view (IGV) obtained from the software NGPINT after Y2H-NGIS analysis of the *Hv*ERdj3B prey reads selected by both the AVR_{A1} and the BEC1016 bait. Prey fragments were reconstructed from the reads mapped to the *HvERdj3B* gene (shown in grey across the exons) in each Y2H-NGIS dataset and located towards the 3' end of the gene in both cases. **C,** Expanded view of the 5' fusion reads that allowed the determination of the frame and nucleotide-resolved prey fragments. The fusion reads contain a prey plasmid sequence (shown in different colors as mismatches from the reference gene) and the prey sequence.

Figure 3. AVR_{A1} and BEC1016 interact with the central part of barley *Hv*ERdj3B in Y2H. **A,** The domains of the 350 aa *Hv*ERdj3B protein and the Y2H-fragments. The signal peptide (SP), the J-domain and the glycine/phenylalanine (G/F)-rich domain are indicated as well as the substrate binding domain predicted according to an alignment with the most closely related mammalian J-domain protein (Chen et al., 2017). Below the three Y2H-fragments are shown. **B,** Yeast transformed with the destination vectors pDEST-AS2-1 (GAL4 binding-domain (BD)) and pDEST-ACT2-1 (GAL4 activation-domain (AD)) (Robertson, 2004) in different combinations of domain-fusions to effectors and the full-length (FL), the central part (centr) and the C-terminal two-thirds (C2/3) of *Hv*ERdj3B. Growth on dropout (DO)-medium lacking leucine (L) and tryptophan (W)

indicated presence of both constructs. Growth on DO-medium lacking L, W, histidine (H) and adenine (A) +/- 2.5 mM 3-amino-1,2,4-triazole (3AT) indicated protein-protein interaction. β-galactosidase assay (X-gal), also indicating protein-protein interaction, was performed on filter paper prints of DO-LW-grown yeast. SNF1/SNF4 was used as a positive control and empty vectors were used as negative control.

Figure 4. Interactions of *Hv*ERdj3B and AVR_{A1} as well as BEC1016 in living plant cells confirmed by BiFC. Reconstitution of fluorescent GFP was observed in *N. benthamiana* epidermal cells expressing the shown combinations of the C and N-terminal parts of GFP fused with *Hv*ERdj3B (w/o SP) and AVR_{A1}/BEC1016 (w/o SP). The remaining combinations did not allow fluorescent GFP to reconstitute (see **Fig. S5**). Expression constructs were introduced using *Agrobacterium* infiltration, and epidermal cells were observed by laser scanning confocal microscopy 48 h later. Size bars, 20 μm.

Figure 5. *Hv*ERdj3B is an ER luminal protein contributing to preinvasive immunity. A, One-week-old barley leaves, bombarded with RNAi and GUS reporter constructs, were inoculated with *Bgh* and scored for fungal haustorium formation, calculated as the ratio of haustoria-containing transformed cells (GUS expressing cells) divided by the total number of transformed cells. Data shown are mean values of four independent experiments. Error bars, SE. Letters (a and b) indicate significant differences calculated using a logistic regression model ($P < 0.001$). **B,** Localization of *Hv*ERdj3B in barley leaf epidermal cells. A ubiquitin promoter-driven expression construct encoding *Hv*ERdj3B (w. SP) fused to the N-terminus of mYFP was co-transformed with an SP-mCherry-HDEL construct into barley epidermal cells using particle bombardment. The cells were observed by confocal laser scanning microscopy 48 h later. **C-F,** Localization of *Hv*ERdj3B in *N. benthamiana* leaf epidermal cells using the split GFP system. *Hv*ERdj3B(w. SP)-GFP11 and SP-GFP1-10-HDEL reconstitute reticulate fluorescent GFP, while GFP11-*Hv*ERdj3B (w/o SP) and GFP1-10 reconstitute cytosolic and nuclear fluorescent GFP. Expression constructs were introduced using *Agrobacterium* infiltration, and epidermal cells were observed by laser scanning confocal microscopy 48 h later. Size bars, 20 μm (B,C,F) and 40 μm (D,E).

Figure 6. AVR_{A1} and BEC1016 localized in the cytosol and nucleus of *N. benthamiana* epidermal cells. Constructs for expression of effectors (w/o SP) were introduced using *Agrobacterium* infiltration, and epidermal cells were observed by laser scanning confocal microscopy 48 h later. Size bars, 40 μm.

Figure 7. AVR_{A1} and BEC1016 are partially translocated into the ER lumen. The GFP1-10/GFP11 self-constituting fluorescence protein demonstrates cytosolic and ER-luminal protein localizations *N. benthamiana* epidermal cells. **A-B and I-J,** GFP11-CNX™ and CNX™-GFP11 confirm SP-GFP11-HDEL to be ER-luminal and GFP1-10 to be cytosolic, respectively. **C-H and K-P,** AVR_{A1}, BEC1016 and CSEP0105 (all w/o SP) are cytosolic while AVR_{A1} and BEC1016 (both w/o SP) are also ER-lumunal, indicated by their reticulate and perinuclear signals (see also **Fig. S8**). Expression constructs were introduced using *Agrobacterium* infiltration, and epidermal cells were observed by laser scanning confocal microscopy 48 h later. Size bars, 40 μm.

Supplemental Figure S1. Attempted alignment of the amino acid sequences of AVR_{A1} (CSEP0008, BLGH_03023) **and BEC1016** (CSEP0491, BLGH_07006)**.** Signal peptides underlined (black), predicted beta sheets underlined (green), and intron position in the encoding genes indicated by dashed line (orange).

Supplemental Figure S2. Transcript accumulation on barley inoculated with *Bgh* isolate 5874. A, *Bgh* effector *AVRa1* (CSEP0008), **B,** *Bgh* effector *BEC1016* (CSEP0491) and **C,** barley target *HvERdj3B* (HORVU1Hr1G022990) in wild-type progenitor CI 16151 (black solid lines) vs. fast-neutron derived susceptible mutant *mla6*-m18982 (dashed red lines). *, significant difference from CI 16151 at an adjusted $P < 0.001$ for barley genes. $P < 0.003$ for *Bgh*.

Supplemental Figure S3. EtHAn-delivery of β-glucuronidase into barley leaf cells. A, Leaf infiltrated with EtHAn transformed with pEDV6-GUS. **B,** non-infiltrated leaf. The two leaves were in parallel incubated in a GUS reaction buffer.

Supplemental Figure S4. Y2H used to validate interactions between AVR_{A1}, BEC1016 and *Hv*ERdj3B. Binary confirmation of the interactions between AVR_{A1}, BEC1016 and *Hv*ERdj3B (aa 132-350), using the binary Y2H system described by Dreze *et al.* (2010) using DO-LW media as diploid control and DO-LWH + 3AT as selection for positive interactions.

Supplemental Figure S5. Bimolecular fluorescence complementation study of the interaction between AVR_{A1}, BEC1016 and *Hv*ERdj3B. These are the non-fluorescent combinations. The fluorescent combinations are shown in **Fig. 4.** See legend of **Fig. 4** for more details. Size bars, 40 µm.

Supplemental Figure S6. Subcellular localization of *Hv*ERdj3B in *N. benthamiana* epidermal cells. *Hv*ERdj3B (w. SP) gave reticular signal overlapping with the SP-mCherry-HDEL ER marker. Size bars, 10 µm.

Supplemental Figure S7. Localization of AVR_{A1} and BEC1016 in barley leaf epidermal cells. Ubiquitin promoter-driven expression constructs encoding SP-free effectors (fused to the C-terminus of mYFP) were co-transformed with a free mCherry construct into barley epidermal cells using particle bombardment. The cells were observed by confocal laser scanning microscopy 48 h later. Size bars, 10 µm.

Supplemental Figure S8. BEC1016 can translocate into the ER. Construct encoding BEC1016-GFP11 (w/o SP) and SP-GFP1-10-HDEL were co-transformed into *N. benthamiana* leaves using *Agrobacterium* infiltration, and epidermal cells were observed by laser scanning confocal microscopy 48 h later. Size bars, 20 µm.

Supplemental Table S1. Y2H-SCORES for the AVRA1 and BEC1016 baits.

Supplemental Table S2. Primer sequences for plasmid constructions (5´ to 3´).

REFERENCES

Aguilar GB, Pedersen C, Thordal-Christensen H (2016) Identification of eight effector candidate genes involved in early aggressiveness of the barley powdery mildew fungus. Plant Pathology **65**: 953-958

Ahmed AA, Pedersen C, Schultz-Larsen T, Kwaaitaal M, Jørgensen HJ, Thordal-Christensen H (2015) The barley powdery mildew candidate secreted effector protein CSEP0105 inhibits the chaperone activity of a small heat shock protein. Plant Physiology **168**: 321-333

Ahmed AA, Pedersen C, Thordal-Christensen H (2016) The barley powdery mildew effector candidates CSEP0081 and CSEP0254 promote fungal infection success. PLoS ONE 11, e0157586.

Banerjee S, Velásquez-Zapata V, Fuerst G, Elmore JM, Wise RP (2021) NGPINT: a next-generation protein–protein interaction software. Briefings in Bioinformatics **22**: bbaa351. DOI: 10.1093/bib/bbaa351

Bauer S, Yu D, Lawson AW, Saur IM, Frantzeskakis L, Kracher B, Logemann E, Chai J, Maekawa T, Schulze-Lefert P (2021) The leucine-rich repeats in allelic barley MLA immune receptors define specificity towards sequence-unrelated powdery mildew avirulence effectors with a predicted common RNase-like fold. PLoS Pathogens **17**: 1-36

Benjamini Y, Hochberg Y 1995. Controlling the false discovery rate: A practical and powerful Approach to multiple testing. J R Stat Soc Ser B. **57**: 289–300.

Bindschedler LV, Burgis TA, Mills DJ, Ho JT, Cramer R, Spanu PD (2009) *In planta* proteomics and proteogenomics of the biotrophic barley fungal pathogen *Blumeria graminis* f. sp. *hordei*. Mol Cell Proteomics **8**: 2368-2381.

Carter ME, Helm M, Chapman AVE, Wan E, Restrepo Sierra AM, Innes RW, Bogdanove AJ, Wise RP (2019) Convergent evolution of effector protease recognition by Arabidopsis and barley. Molecular Plant-Microbe Interactions **32**: 550-565.

Chapman AVE, Hunt M, Surana P, Velásquez-Zapata V, Xu W, Fuerst G, Wise RP (2021) Disruption of barley immunity to powdery mildew by an in-frame Lys-Leu deletion in the essential protein SGT1. Genetics **217**: iyaa026.

Chen KC, Qu S, Chowdhury S, Noxon IC, Schonhoft JD, Plate L, Powers ET, Kelly JW, Lander GC, Wiseman RL (2017) The endoplasmic reticulum HSP 40 co-chaperone ERdj3/DNAJB11 assembles and functions as a tetramer. EMBO Journal **36**: 2296-2309

Douchkov D, Nowara D, Zierold U, Schweizer P (2005) A high-throughput gene-silencing system for the functional assessment of defense-related genes in barley epidermal cells. Molecular Plant-Microbe Interactions **18**: 755-761

Dreze M, Monachello D, Lurin C, Cusick ME, Hill DE, Vidal M, Braun P (2010) High-quality binary interactome mapping. Methods in Enzymology **470**: 281-315

Erffelinck ML, Ribeiro B, Perassolo M, Pauwels L, Pollier J, Storme V, Goossens A (2018) A user-friendly platform for yeast two-hybrid library screening using next generation sequencing. PLoS One **13**: 1-21

Fabro G, Steinbrenner J, Coates M, Ishaque N, Baxter L, Studholme DJ, Körner E, Allen RL, Piquerez SJ, Rougon-Cardoso A, Greenshields D, et al. (2011) Multiple candidate effectors from

the oomycete pathogen *Hyaloperonospora arabidopsidis* suppress host plant immunity. PLoS Pathogen **7**: 1-18

Fan G, Yang Y, Li T, Lu W, Du Y, Qiang X, Wen Q, Shan W (2018) A *Phytophthora capsici* RXLR effector targets and inhibits a plant PPIase to suppress endoplasmic reticulum-mediated immunity. Molecular Plant **11**: 1067-1083

Fatima K, Naqvi F, Younas H (2021) A Review: Molecular Chaperone-mediated Folding, Unfolding and Disaggregation of Expressed Recombinant Proteins. Cell Biochemistry and Biophysics **79**: 153-174

Figueroa M, Ortiz D, Henningsen EC (2021) Tactics of host manipulation by intracellular effectors from plant pathogenic fungi. Currernt Opinion in Plant Biololgy **62**: 102054

Frantzeskakis L, Kracher B, Kusch S, Yoshikawa-Maekawa M, Bauer S, Pedersen C, Spanu PD, Maekawa T, Schulze-Lefert P, Panstruga R (2018) Signatures of host specialization and a recent transposable element burst in the dynamic one-speed genome of the fungal barley powdery mildew pathogen. BMC Genomics **19**: 1-23

Hu CD, Kerppola TK (2003) Simultaneous visualization of multiple protein interactions in living cells using multicolor fluorescence complementation analysis. Nature Biotechnology **21**: 539-545

Hunt M, Banerjee S, Surana P, Liu M, Fuerst G, Mathioni S, Meyers BC, Nettleton D, Wise RP (2019) Small RNA discovery in the interaction between barley and the powdery mildew pathogen. BMC Genomics **20**: 610.

Jin L, Mackey DM (2017) Measuring callose deposition, an indicator of cell wall reinforcement, during bacterial infection in Arabidopsis. Methods in Molecular Biology 1578: 195-205

Jing M, Guo B, Li H, Yang B, Wang H, Kong G, Zhao Y, Xu H, Wang Y, Ye W, Dong S, et al. (2016) A *Phytophthora sojae* effector suppresses endoplasmic reticulum stress-mediated immunity by stabilizing plant binding immunoglobulin proteins. Nature Communications **7**: 1-17

Jones JD, Vance RE, Dangl JL (2016) Intracellular innate immune surveillance devices in plants and animals. Science **354**: aaf6395

Kamigaki A, Nito K, Hikino K, Goto-Yamada S, Nishimura M, Nakagawa T, Mano S (2016) Gateway vectors for simultaneous detection of multiple protein−protein interactions in plant cells using bimolecular fluorescence complementation. PLoS One **11:** e0160717.

Kanja C, Hammond-Kosack KE (2020) Proteinaceous effector discovery and characterization in filamentous plant pathogens. Molecular Plant Pathology **21**: 1353-1376

Keselman HJ, Algina J, Kowalchuk RK (2001) The analysis of repeated measures designs: A review. Br J Math Stat Psychol. **54**: 1**–**20.

Kourelis J, Van Der Hoorn RA (2018) Defended to the nines: 25 years of resistance gene cloning identifies nine mechanisms for R protein function. Plant Cell **30**: 285-299

Kørner CJ, Du X, Vollmer ME, Pajerowska-Mukhtar KM (2015) Endoplasmic reticulum stress signaling in plant immunity-at the crossroad of life and death. International Journal of Molecular Sciences **16**: 26582-26598

Lewis JD, Wan J, Ford R, Gong Y, Fung P, Nahal H, Wang PW, Desveaux D, Guttman DS (2012)

Quantitative Interactor Screening with next-generation Sequencing (QIS-Seq) identifies *Arabidopsis thaliana* MLO2 as a target of the *Pseudomonas syringae* type III effector HopZ2. BMC Genomics **13**: 1-13

Li J, Zhao-Hui C, Batoux M, Nekrasov V, Roux M, Chinchilla D, Zipfel C, Jones JD (2009) Specific ER quality control components required for biogenesis of the plant innate immune receptor EFR. Proceedings of the National Academy of Sciences USA **106**: 15973-15978

Li X, Jin C, Yuan H, Huang W, Liu F, Fan R, Xie J, Shen QH (2021) The barley powdery mildew effectors CSEP0139 and CSEP0182 suppress cell death and promote *B. graminis* fungal virulence in plants. Phytopathology Research **3**: 1-14

Lu X, Kracher B, Saur IM, Bauer S, Ellwood SR, Wise R, Yaeno T, Maekawa T, Schulze-Lefert P (2016) Allelic barley MLA immune receptors recognize sequence-unrelated avirulence effectors of the powdery mildew pathogen. Proceedings of the National Academy of Sciences USA **113**: E6486-E6495

Lück S, Kreszies T, Strickert M, Schweizer P, Kuhlmann M, Douchkov D (2019) siRNA-Finder (si-Fi) software for RNAi-target design and off-target prediction. Frontiers in Plant Science **10**: 1023

Menardo F, Praz CR, Wicker T, Keller B (2017) Rapid turnover of effectors in grass powdery mildew (*Blumeria graminis*). BMC Evolutionary Biology **17**: 1-14

Moreno AA, Mukhtar MS, Blanco F, Boatwright JL, Moreno I, Jordan MR, Chen Y, Brandizzi F, Dong X, Orellana A, Pajerowska-Mukhtar KM (2012) IRE1/bZIP60-mediated unfolded protein response plays distinct roles in plant immunity and abiotic stress responses. PLoS One **7**: 1-15

Mukhtar MS, Carvunis AR, Dreze M, Epple P, Steinbrenner J, Moore J, Tasan M, Galli M, Hao T, Nishimura MT, Pevzner SJ (2011) Independently evolved virulence effectors converge onto hubs in a plant immune system network. Science **333**: 596-601

Nekrasov V, Li J, Batoux M, Roux M, Chu ZH, Lacombe S, Rougon A, Bittel P, Kiss-Papp M, Chinchilla D, Van Esse HP, et al. (2009) Control of the pattern-recognition receptor EFR by an ER protein complex in plant immunity. EMBO Journal **28**: 3428-3438

Nelson BK, Cai X, Nebenführ A (2007) A multicolored set of in vivo organelle markers for co-localization studies in Arabidopsis and other plants. Plant Journal **51**: 1126-1136

Ngou BPM, Ding P, Jones JD (2022) Thirty years of resistance: Zig-zag through the plant immune system. Plant Cell doi: 10.1093/plcell/koac041

Nowara D, Gay A, Lacomme C, Shaw J, Ridout C, Douchkov D, Hensel G, Kumlehn J, Schweizer P (2010) HIGS: host-induced gene silencing in the obligate biotrophic fungal pathogen *Blumeria graminis*. Plant Cell **22**: 3130-3141

Pashkova N, Peterson TA, Krishnamani V, Breheny P, Stamnes M, Piper RC (2016) DEEPN as an approach for batch processing of yeast 2-hybrid interactions. Cell Reports **17**: 303-315

Pedersen C, van Themaat EV, McGuffin LJ, Abbott JC, Burgis TA, Barton G, Bindschedler LV, Lu X, Maekawa T, Weßling R, Cramer R, et al. (2012) Structure and evolution of barley powdery mildew effector candidates. BMC Genomics **13**: 1-21

Pennington HG, Jones R, Kwon S, Bonciani G, Thieron H, Chandler T, Luong P, Morgan SN, Przydacz M, Bozkurt T, Bowden S, et al. (2019) The fungal ribonuclease-like effector protein

CSEP0064/BEC1054 represses plant immunity and interferes with degradation of host ribosomal RNA. PLoS Pathogens **15**: 1-33

Pliego C, Nowara D, Bonciani G, Gheorghe DM, Xu R, Surana P, Whigham E, Nettleton D, Bogdanove AJ, Wise RP, Schweizer P, et al. (2013) Host-induced gene silencing in barley powdery mildew reveals a class of ribonuclease-like effectors. Molecular Plant-Microbe Interactions **26**: 633-642

Pobre KF, Poet GJ, Hendershot LM (2019) The endoplasmic reticulum (ER) chaperone BiP is a master regulator of ER functions: Getting by with a little help from ERdj friends. Journal of Biological Chemistry **294**: 2098-2108

Qiang X, Zechmann B, Reitz MU, Kogel KH, Schäfer P (2012) The mutualistic fungus Piriformospora indica colonizes Arabidopsis roots by inducing an endoplasmic reticulum stress–triggered caspase-dependent cell death. Plant Cell **24**: 794-809

Rasco-Gaunt S, Riley A, Barcelo P, Lazzeri PA (1999) Analysis of particle bombardment parameters to optimise DNA delivery into wheat tissues. Plant Cell Reports **19**: 118-127

Robertson M (2004) Two transcription factors are negative regulators of gibberellin response in the HvSPY-signaling pathway in barley aleurone. Plant Physiology **136**: 2747-2761

Saur IM, Bauer S, Kracher B, Lu X, Franzeskakis L, Müller MC, Sabelleck B, Kümmel F, Panstruga R, Maekawa T, Schulze-Lefert P (2019) Multiple pairs of allelic MLA immune receptor-powdery mildew AVR_A effectors argue for a direct recognition mechanism. Elife **8**: 1-31

Schindelin J, Arganda-Carreras I, Frise E, Kaynig V, Longair M, Pietzsch T, Preibisch S, Rueden C, Saalfeld S, Schmid B, Tinevez JY, et al. (2012) Fiji: an open-source platform for biological-image analysis. Nat Methods. **9:** 676-82

Seeholzer S, Tsuchimatsu T, Jordan T, Bieri S, Pajonk S, Yang W, Jahoor A, Shimizu KK, Keller B, Schulze-Lefert P (2010) Diversity at the *Mla* powdery mildew resistance locus from cultivated barley reveals sites of positive selection. Molecular Plant-Microbe Interactions **23**: 497-509

Sivamani E, DeLong RK, Qu R (2009) Protamine-mediated DNA coating remarkably improves bombardment transformation efficiency in plant cells. Plant Cell Reports **28**: 213-221

Sohn KH, Lei R, Nemri A, Jones JD (2007) The downy mildew effector proteins ATR1 and ATR13 promote disease susceptibility in Arabidopsis thaliana. Plant Cell **19**: 4077-4090

Spanu PD, Abbott JC, Amselem J, Burgis TA, Soanes DM, et al. (2010). Genome expansion and gene loss in powdery mildew fungi reveal tradeoffs in extreme parasitism. Science **330**: 1543-1546.

Spanu PD (2017). Cereal immunity against powdery mildews targets RNase-Like Proteins associated with Haustoria (RALPH) effectors evolved from a common ancestral gene. New Phytologist **213:** 969-971

Sun Y, Zhu YX, Balint-Kurti PJ, Wang GF (2020) Fine-tuning immunity: players and regulators for plant NLRs. Trends in Plant Science **25**: 695-713

Surana P (2017) Membrane trafficking in resistance gene-mediated defense against the barley powdery mildew fungus (Doctoral dissertation, Iowa State University)

Suter B, Zhang X, Pesce CG, Mendelsohn AR, Dinesh-Kumar SP, Mao JH (2015) Next-generation sequencing for binary protein–protein interactions. Frontiers in Genetics **6:** 1-6

Thomas WJ, Thireault CA, Kimbrel JA, Chang JH (2009) Recombineering and stable integration of the Pseudomonas syringae pv. syringae 61 hrp/hrc cluster into the genome of the soil bacterium *Pseudomonas fluorescens* Pf0-1. Plant Journal **60:** 919-928

Thordal-Christensen H (2020) A holistic view on plant effector-triggered immunity presented as an iceberg model. Cellular and Molecular Life Sciences **10:** 1-14

Tintor N, Saijo Y (2014) ER-mediated control for abundance, quality, and signaling of transmembrane immune receptors in plants. Frontiers in Plant Science **5:** 65

Trigg SA, Garza RM, MacWilliams A, Nery JR, Bartlett A, Castanon R, Goubil A, Feeney J, O'Malley R, Shao-shan CH, Zhang ZZ, et al. (2017) CrY2H-seq: a massively multiplexed assay for deep-coverage interactome mapping. Nature Methods **14:** 819-825

Upadhyaya NM, Ellis JG, Dodds PN (2014) A bacterial type III secretion-based delivery system for functional assays of fungal effectors in cereals. Methods in Molecular Biology **1127:** 277-290

van Wersch S, Tian L, Hoy R, Li X (2020) Plant NLRs: the whistleblowers of plant immunity. Plant Communications **1:** 100016

Velásquez-Zapata V, Elmore JM, Banerjee S, Dorman KS, Wise RP (2021) Next-generation yeast-two-hybrid analysis with Y2H-SCORES identifies novel interactors of the MLA immune receptor. PLoS Computational Biology **17:** e1008890. DOI: 10.1371/journal.pcbi.1008890

Velásquez-Zapata V, Elmore JM, Fuerst GS, Wise RP (2022) An interolog-based barley interactome as an integration framework for NLR immune signaling. Genetics: iyac056, https://doi.org/10.1093/genetics/iyac056.

Voigt CA (2014) Callose-mediated resistance to pathogenic intruders in plant defense-related papillae. Frontiers in Plant Science **5:** 168

Voigt CA (2016) Cellulose/callose glucan networks: the key to powdery mildew resistance in plants? New Phytologist **212:** 303-305

Voinnet O, Rivas S, Mestre P, Baulcombe D (2003) Retracted: An enhanced transient expression system in plants based on suppression of gene silencing by the p19 protein of tomato bushy stunt virus. Plant Journal **33:** 949-956

Wang J, Dhroso A, Liu X, Baum TJ, Hussey RS, Davis EL, Wang X, Korkin D, Mitchum MG (2021) Phytonematode peptide effectors exploit a host post-translational trafficking mechanism to the ER using a novel translocation signal. New Phytologist **229:** 563-574

Wang Z, Li X, Wang X, Liu N, Xu B, Peng Q, Guo Z, Fan B, Zhu C, Chen Z (2019) Arabidopsis endoplasmic reticulum-localized UBAC2 proteins interact with PAMP-INDUCED COILED-COIL to regulate pathogen-induced callose deposition and plant immunity. Plant Cell **31**: 153-171

Weimann M, Grossmann A, Woodsmith J, Özkan Z, Birth P, Meierhofer D, Benlasfer N, Valovka T, Timmermann B, Wanker EE, Sauer S (2013) A Y2H-seq approach defines the human protein methyltransferase interactome. Nature Methods **10**: 339-342

Weßling R, Epple P, Altmann S, He Y, Yang L, Henz SR, McDonald N, Wiley K, Bader KC, Gläßer C,

Mukhtar MS, et al. (2014) Convergent targeting of a common host protein-network by pathogen effectors from three kingdoms of life. Cell Host & Microbe **16**: 364-375

Xie W, Nielsen ME, Pedersen C, Thordal-Christensen H (2017) A split-GFP gateway cloning system for topology analyses of membrane proteins in plants. PloS One **12**: 1-8

Xu Q, Tang C, Wang L, Zhao C, Kang Z, Wang X (2020) Haustoria-arsenals during the interaction between wheat and *Puccinia striiformis* f. sp. *tritici*. Molecular Plant Pathology **21**: 83-94

Xu W, Meng Y, Surana P, Fuerst G, Nettleton D, Wise RP (2015) The knottin-like Blufensin family regulates genes involved in nuclear import and the secretory pathway in barley-powdery mildew interactions. Frontiers in Plant Science **6:** 409.

Xu G, Zhong X, Shi Y, Liu Z, Jiang N, Liu J, Ding B, Li Z, Kang H, Ning Y, Liu W, et al. (2020) A fungal effector targets a heat shock–dynamin protein complex to modulate mitochondrial dynamics and reduce plant immunity. Science Advances **6**: 1-10.

Yachie N, Petsalaki E, Mellor JC, Weile J, Jacob Y, Verby M, Ozturk SB, Li S, Cote AG, Mosca R, Knapp JJ, et al. (2016) Pooled-matrix protein interaction screens using Barcode Fusion Genetics. Molecular Systems Biology **12:** 863

Yamamoto M, Maruyama D, Endo T, Nishikawa SI (2008) *Arabidopsis thaliana* has a set of J proteins in the endoplasmic reticulum that are conserved from yeast to animals and plants. Plant and Cell Physiology **49**: 1547-1562

Yu CP, Chen SC, Chang YM, Liu WY, Lin HH, Lin JJ, Chen HJ, Lu YJ, Wu YH, Lu MY, Lu CH, et al. (2015) Transcriptome dynamics of developing maize leaves and genomewide prediction of cis elements and their cognate transcription factors. Proceedings of the National Academy of Sciences USA **112**: E2477-E2486

Yuan M, Jiang Z, Bi G, Nomura K, Liu M, Wang Y, Cai B, Zhou JM, He SY, Xin XF (2021a) Pattern-recognition receptors are required for NLR-mediated plant immunity. Nature **592**: 105-109

Yuan H, Jin C, Pei H, Zhao L, Li X, Li J, Huang W, Fan R, Liu W, Shen QH (2021b) The powdery mildew effector CSEP0027 interacts with barley catalase to regulate host immunity. Front Plant Sci. **12:** 733237

Zhang WJ, Pedersen C, Kwaaitaal M, Gregersen PL, Mørch SM, Hanisch S, Kristensen A, Fuglsang AT, Collinge DB, Thordal-Christensen H (2012) Interaction of barley powdery mildew effector candidate CSEP0055 with the defence protein PR17c. Molecular Plant Pathology **13**: 1110-1119.

Zhang W-J, Hanisch S, Kwaaitaal M, Pedersen C, Thordal-Christensen H (2013) A component of the Sec61 ER protein transporting pore is required for plant susceptibility to powdery mildew. Frontiers in Plant Science **4:** 127

Zhong X, Yang J, Shi Y, Wang X, Wang GL (2018) The DnaJ protein OsDjA6 negatively regulates rice innate immunity to the blast fungus *Magnaporthe oryzae*. Molecular Plant Pathology **19**: 607-614

Zimmermann R, Eyrisch S, Ahmad M, Helms V (2021) Protein translocation across the ER membrane. Biochimica et Biophysica Acta **1808:** 912–924

Zipfel C, Oldroyd GE (2017) Plant signalling in symbiosis and immunity. Nature **543**: 328-336

Powdery mildew effectors AVR_{A1} and BEC1016 target the ER J-domain protein *Hv*ERdj3B required for immunity in barley

Figure 1

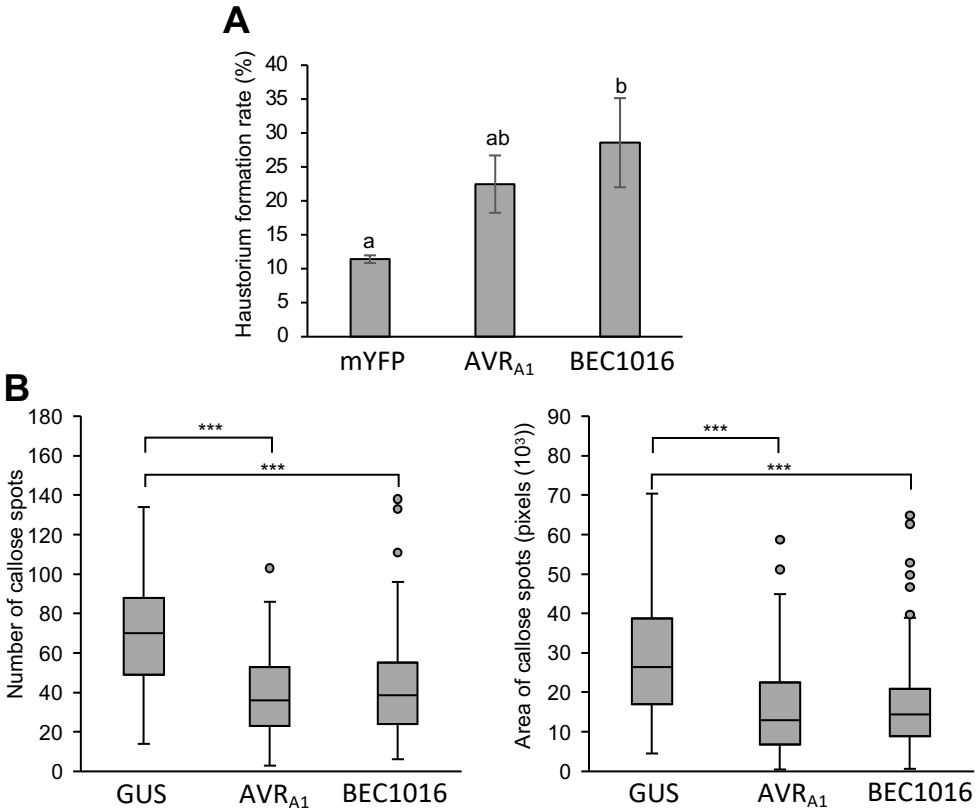

Figure 1. Influence of AVR_{A1} and BEC1016 on *Bgh* infection and callose deposition in barley. A, Effect of transient over-expression of AVR_{A1} and BEC1016 on *Bgh* invasion. pUbi promoter-driven over-expression constructs were co-bombarded with a GUS-reporter constructs into leaf epidermal cells of 1-week-old barley and 2 days later inoculated with *Bgh*. After another 2 days, the fungal haustorium formation was scored in GUS expressing cells. Data shown are mean values of three independent experiments. Error bars, SE. Letters (a, ab and b) indicate significant differences calculated using a logistic regression model (P = 0.0179). **B,** AVR_{A1} and BEC1016 can reduce bacterium-triggered callose deposition in barley plants estimated as numbers of callose spots (left) and area of callose spots (right). Leaves of eight-day-old barley plants were infiltrated with EtHAn, transformed with pEDV6-GUS, pEDV6-AVR_{A1} or pEDV6-BEC1016, and 24 h later the callose deposition we scored. Boxplots for the total number and total area of callose depositions show data for all pictures taken across biological replicates under each treatment. A repeated measures ANOVA followed for a paired sample t test were used to compare the treatments. ***, $P < 2x10^{-16}$. Data shown are based on five independent experiments, statistically treated as replicates.

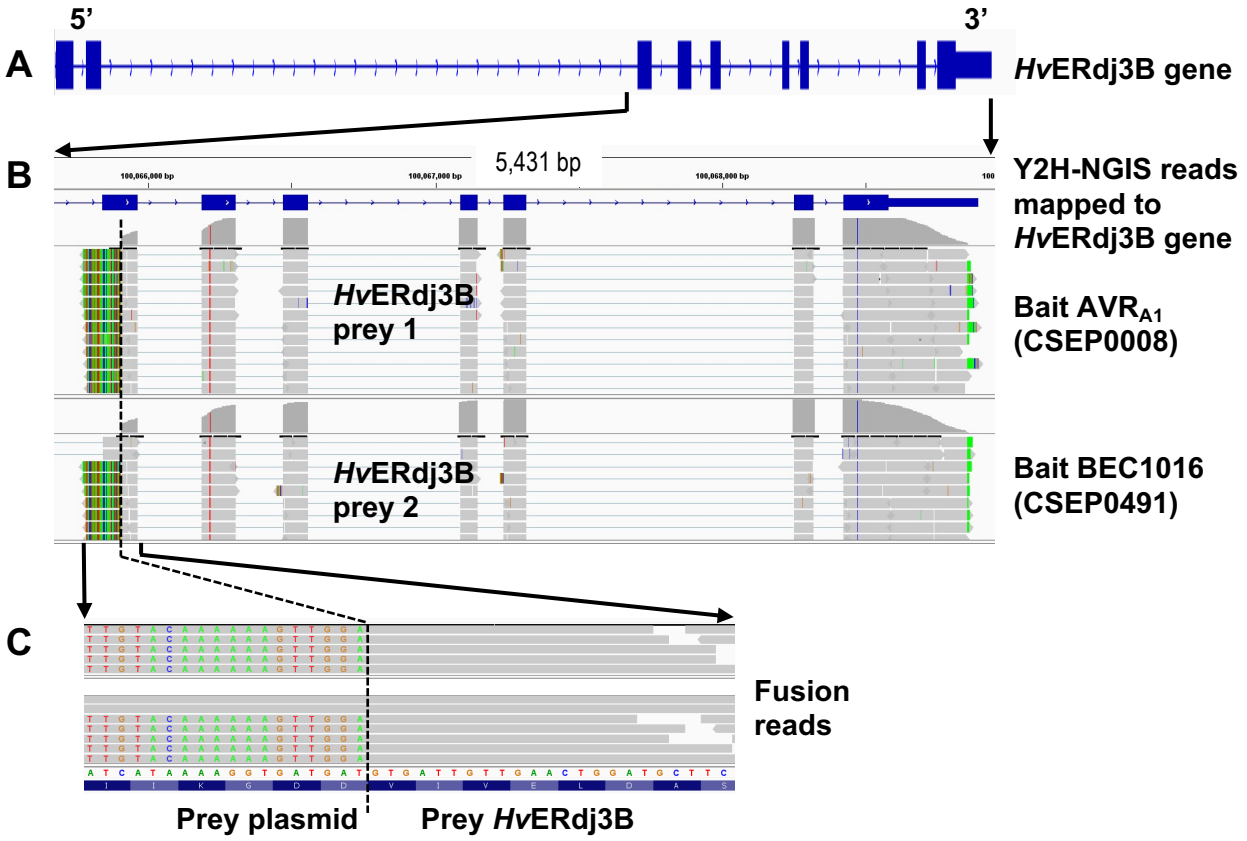

Figure 2. Y2H-NGIS used to identify interactions between AVR_{A1}, BEC1016 and *Hv*ERdj3B. A, *Hv*ERdj3B gene model with exons depicted as blue boxes and introns as hash marks. **B,** Integrative genomic view (IGV) obtained from the software NGPINT after Y2H-NGIS analysis of the *Hv*ERdj3B prey reads selected by both the AVR_{A1} and the BEC1016 bait. Prey fragments were reconstructed from the reads mapped to the *HvERdj3B* gene (shown in grey across the exons) in each Y2H-NGIS dataset and located towards the 3' end of the gene in both cases. **C,** Expanded view of the 5' fusion reads that allowed the determination of the frame and nucleotide-resolved prey fragments. The fusion reads contain a prey plasmid sequence (shown in different colors as mismatches from the reference gene) and the prey sequence.

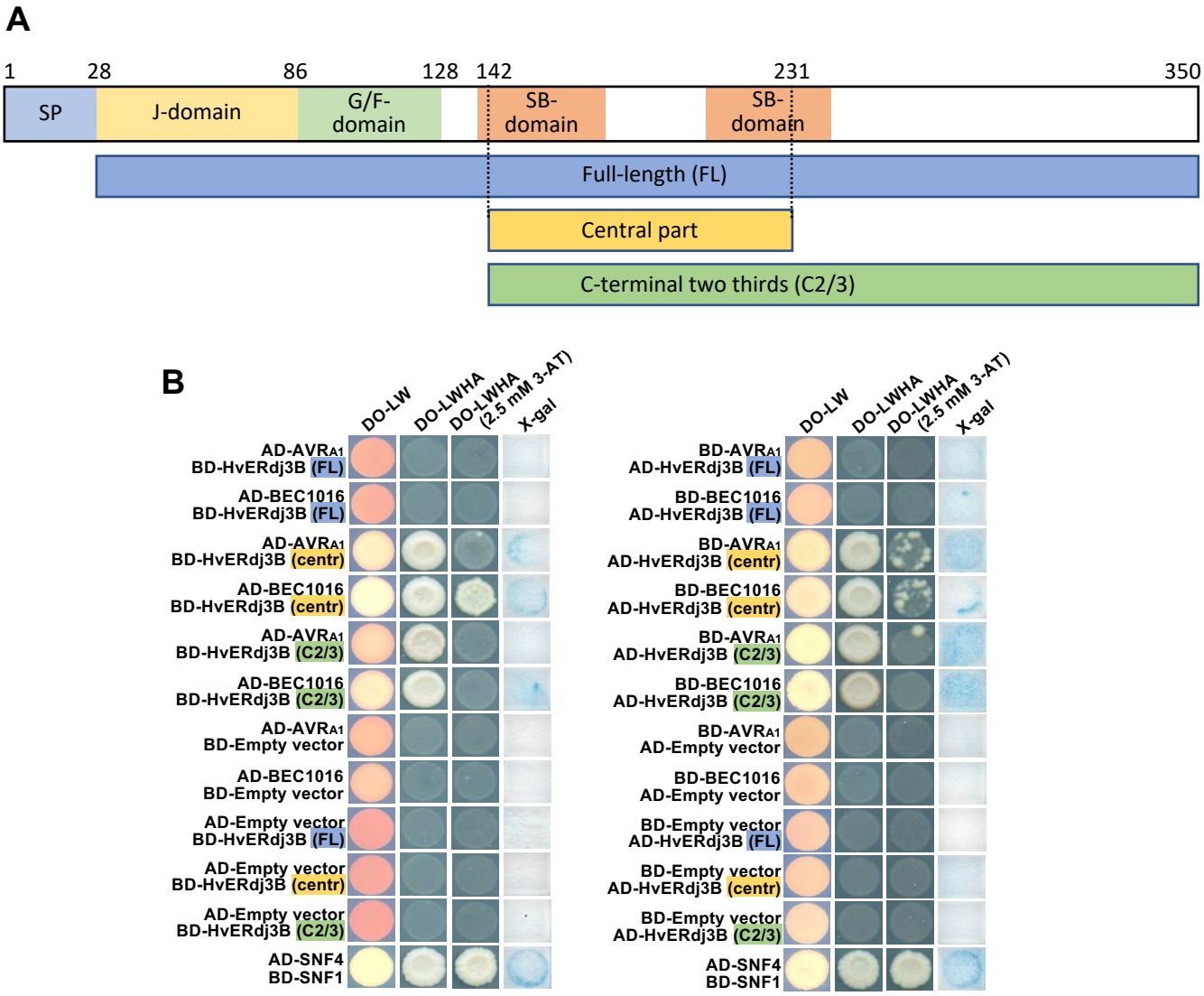

Figure 3. AVR_{A1} and BEC1016 interact with the central part of barley *Hv*ERdj3B in Y2H. **A,** The domains of the 350 aa *Hv*ERdj3B protein and the Y2H-fragments. The signal peptide (SP), the J-domain and the glycine/phenylalanine (G/F)-rich domain are indicated as well as the substrate binding domain predicted according to an alignment with the most closely related mammalian J-domain protein (Chen et al., 2017). Below the three Y2H-fragments are shown. **B,** Yeast transformed with the destination vectors pDEST-AS2-1 (GAL4 binding-domain (BD)) and pDEST-ACT2-1 (GAL4 activation-domain (AD)) (Robertson, 2004) in different combinations of domain-fusions to effectors and the full-length (FL), the central part (centr) and the C-terminal two-thirds (C2/3) of *Hv*ERdj3B. Growth on dropout (DO)-medium lacking leucine (L) and tryptophan (W) indicated presence of both constructs. Growth on DO-medium lacking L, W, histidine (H) and adenine (A) +/- 2.5 mM 3-amino-1,2,4-triazole (3AT) indicated protein-protein interaction. β-galactosidase assay (X-gal), also indicating protein-protein interaction, was performed on filter paper prints of DO-LW-grown yeast. SNF1/SNF4 was used as a positive control and empty vectors were used as negative control.

Figure 4

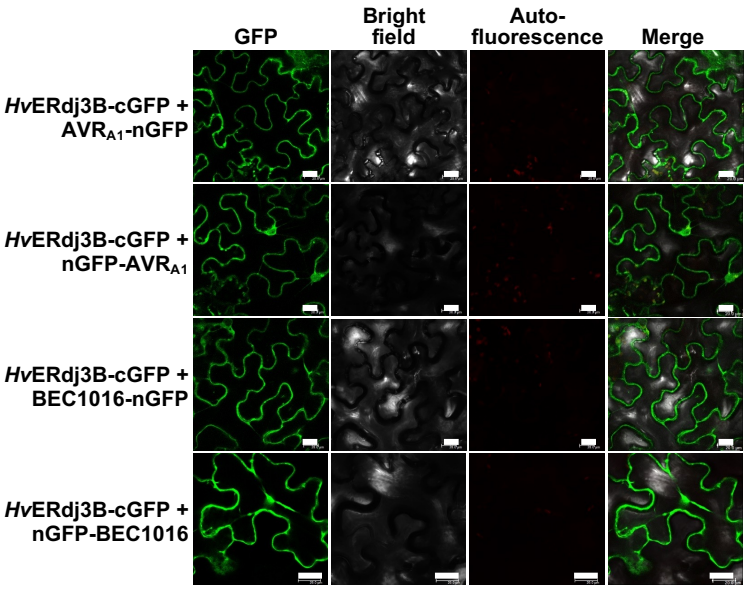

Figure 4. Interactions of *Hv*ERdj3B and AVR$_{A1}$ as well as BEC1016 in living plant cells confirmed by BiFC. Reconstitution of fluorescent GFP was observed in *N. benthamiana* epidermal cells expressing the shown combinations of the C and N-terminal parts of GFP fused with *Hv*ERdj3B (w/o SP) and AVR$_{A1}$/BEC1016 (w/o SP). The remaining combinations did not allow fluorescent GFP to reconstitute (see **Fig. S5**). Expression constructs were introduced using *Agrobacterium* infiltration, and epidermal cells were observed by laser scanning confocal microscopy 48 h later. Size bars, 20 μm.

Figure 5

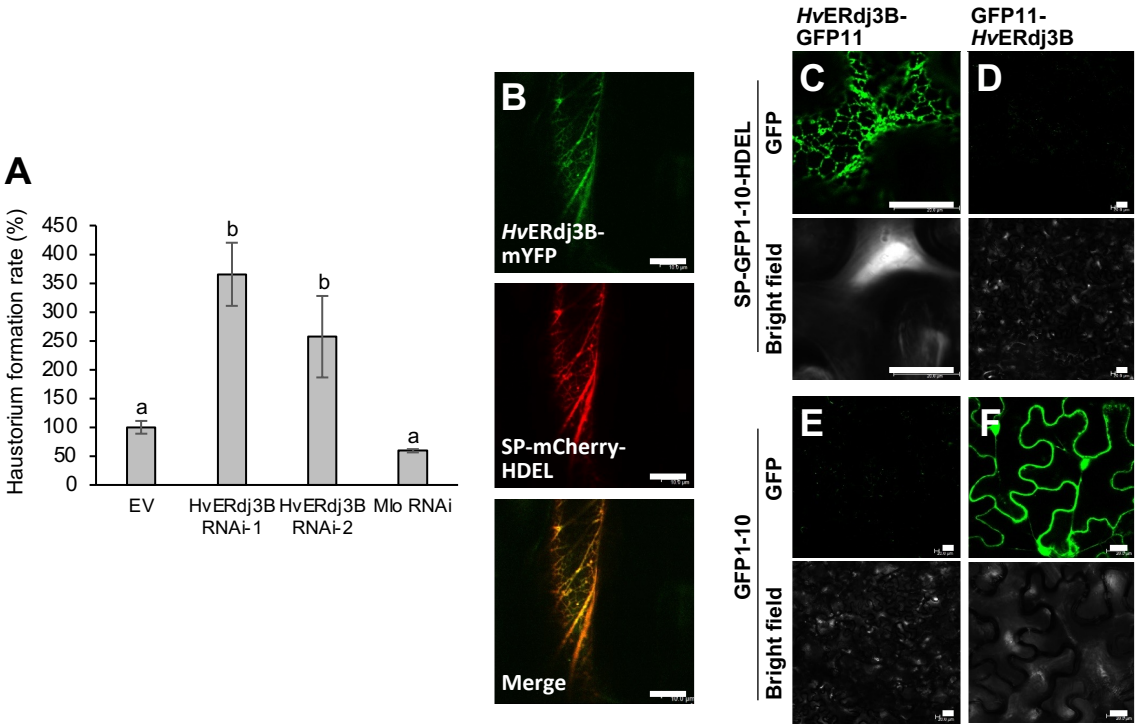

Figure 5. *Hv*ERdj3B is an ER luminal protein contributing to preinvasive immunity. A, One-week-old barley leaves, bombarded with RNAi and GUS reporter constructs, were inoculated with *Bgh* and scored for fungal haustorium formation, calculated as the ratio of haustoria-containing transformed cells (GUS expressing cells) divided by the total number of transformed cells. Data shown are mean values of four independent experiments. Error bars, SE. Letters (a and b) indicate significant differences calculated using a logistic regression model ($P < 0.001$). **B,** Localization of *Hv*ERdj3B in barley leaf epidermal cells. A ubiquitin promoter-driven expression construct encoding *Hv*ERdj3B (w. SP) fused to the N-terminus of mYFP was co-transformed with an SP-mCherry-HDEL construct into barley epidermal cells using particle bombardment. The cells were observed by confocal laser scanning microscopy 48 h later. **C-F,** Localization of *Hv*ERdj3B in *N. benthamiana* leaf epidermal cells using the split GFP system. *Hv*ERdj3B(w. SP)-GFP11 and SP-GFP1-10-HDEL reconstitute reticulate fluorescent GFP, while GFP11-*Hv*ERdj3B (w/o SP) and GFP1-10 reconstitute cytosolic and nuclear fluorescent GFP. Expression constructs were introduced using *Agrobacterium* infiltration, and epidermal cells were observed by laser scanning confocal microscopy 48 h later. Size bars, 20 μm (B,C,F) and 40 μm (D,E).

Figure 6

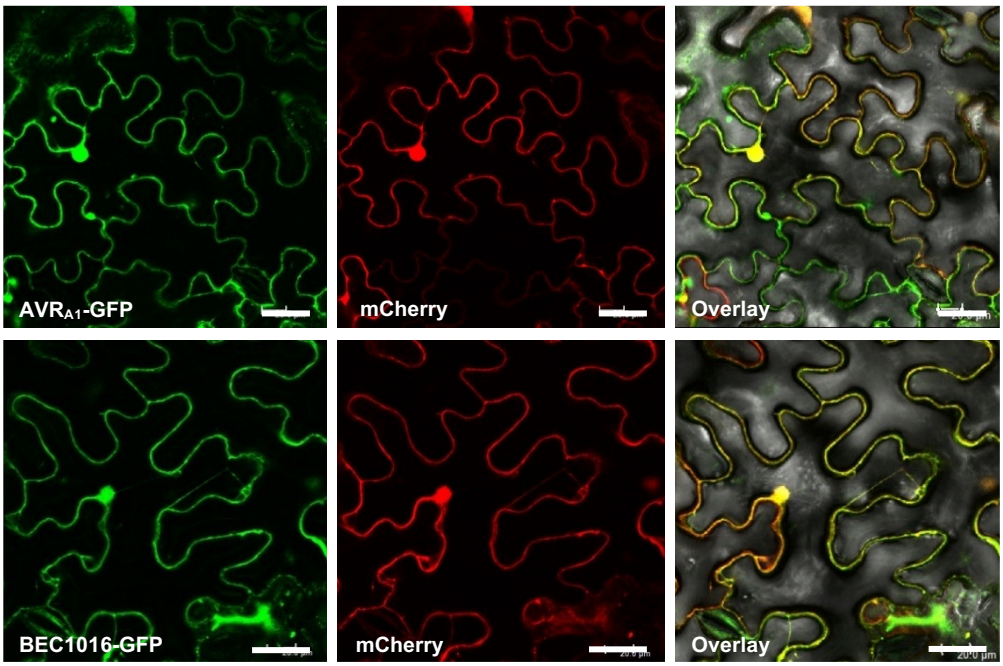

Figure 6. AVR$_{A1}$ and BEC1016 localized in the cytosol and nucleus of *N. benthamiana* epidermal cells. Constructs for expression of effectors (w/o SP) were introduced using *Agrobacterium* infiltration, and epidermal cells were observed by laser scanning confocal microscopy 48 h later. Size bars, 40 μm.

Figure 7

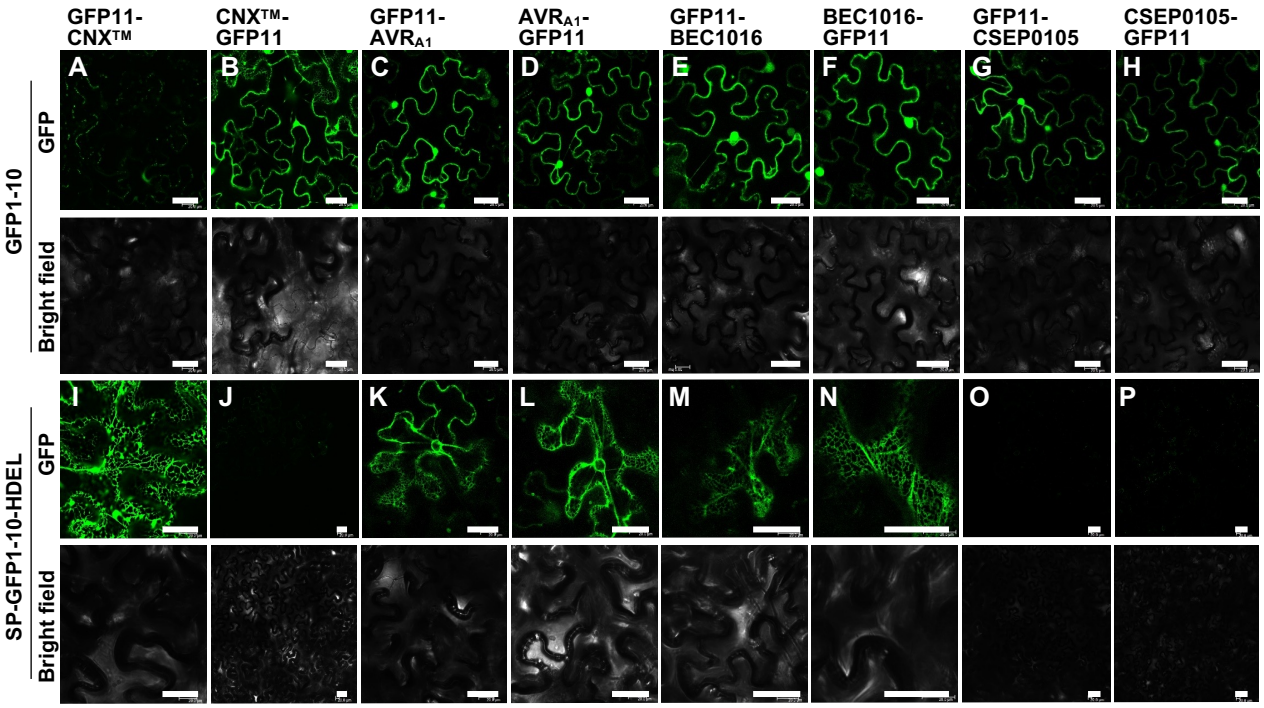

Figure 7. AVR_{A1} and BEC1016 are partially translocated into the ER lumen. The GFP1-10/GFP11 self-constituting fluorescence protein demonstrates cytosolic and ER-luminal protein localizations *N. benthamiana* epidermal cells. **A-B and I-J,** GFP11-CNX^{TM} and CNX^{TM}-GFP11 confirm SP-GFP11-HDEL to be ER-luminal and GFP1-10 to be cytosolic, respectively. **C-H and K-P,** AVR_{A1}, BEC1016 and CSEP0105 (all w/o SP) are cytosolic while AVR_{A1} and BEC1016 (both w/o SP) are also ER-lumunal, indicated by their reticulate and perinuclear signals (see also **Fig. S8**). Expression constructs were introduced using *Agrobacterium* infiltration, and epidermal cells were observed by laser scanning confocal microscopy 48 h later. Size bars, 40 μm.